# Teleoperated Steering Using Estimated Position and Orientation of Remote Ego Vehicle\*

Gaurav Sharma and Rajesh Rajamani

Abstract— Teleoperation of a vehicle requires displaying the road environment of the remote vehicle accurately on a teleoperation station, so that a human teleoperator can use the display to control the vehicle safely and efficiently. Limited bandwidth and latencies in wireless communication may prevent transmission of camera images and Lidar data at a sufficiently high frequency for rapid updates of the display. This paper describes how frequent transmission of just GPS and IMU data can enable accurate vehicle position and orientation estimation with which realistic intermediate updates of the remote vehicle environment can be provided. A nonlinear dynamic motion model and an extended Kalman filter are utilized for estimating vehicle position and orientation. A study with 5 human subjects is used to compare steering control of a remote vehicle with and without intermediate position updates. Experimental data show that a 0.5 second delay in real-time display makes it extremely difficult for a human teleoperator to control the vehicle to stay in its lane on curved roads. However, using an estimation-based predictive display system to update the vehicle position and orientation with respect to the road environment enables safe remote vehicle control with almost as accurate a performance as the delay-free case.

## I. INTRODUCTION

Teleoperation is currently used effectively for controlling delivery robots on many campuses and in limited urban locations [1]. Such teleoperation could similarly play a role in the future in enabling remote take-over of an autonomous vehicle when such human intervention is found to be necessary. Some examples of situations where human intervention may be needed are the presence of snow cover on the road making the lane markers invisible, active snow/rain precipitation, the presence of construction zones on road, and the failure of critical sensors, actuators or other components on the vehicle. Currently, such human intervention is provided by using backup safety drivers who are almost always present as a part of autonomous vehicles during testing. Instead, a remote teleoperator could be used to step in and get the car past whatever hazard might be too hard for the vehicle to handle by itself in an autonomous fashion.

Teleoperation requires strong wireless connectivity between the autonomous vehicle and a teleoperation station. Camera images and data from the car can then be transmitted to the teleoperation to recreate the road environment of the remote vehicle for the human teleoperator. Due to the large data streams associated with camera and Lidar measurements,

\* Research supported in part by the University of Minnesota InterS&Ections Program and by NSF Grant CNS 2321531.

frequent transmission of such data at rapid update rates is a challenge.

Delayed perception during teleoperated driving significantly increases the effort of the human, and the operator has to take care of the task and the monitoring of the environment with more intensive effort [2,3]. This paper proposes to develop an estimation based predictive display system that estimates trajectories of the ego vehicle to perform realistic intermediate updates of the vehicle with respect to its remote environment to compensate for delayed camera data.

Previous researchers have studied several approaches to the display of predicted ego-vehicle position on the teleoperator screen. Approaches studied include the use of a semitransparent vehicle [4], a rectangular frame and tracks [5] or a pointing line [6] on the display screen to indicate the predicted position of the vehicle. However, they just assumed the ego-vehicle position was known and did not study how the remote vehicle position could actually be estimated. Other researchers have used open-loop predictions of future motion to predict ego vehicle position, based on assumptions such as clothoid trajectories [7,8] and predictors for the vehicle motion [9]. Finally, researchers have also used zooming and sliding (or image transformation) on the display based on data from real-time throttle/brake/steering inputs of the teleoperator [10,11]. However, none of the authors described above have used model-based estimation algorithms for prediction of ego-vehicle position.

This paper utilizes a nonlinear dynamic model of the vehicle motion and an extended Kalman filter to estimate the remote vehicle's position and orientation. It is assumed that the vehicle is able to transmit GNSS and IMU data frequently at an update of 100 Hz, while camera images from the vehicle arrive with a time-delay of 0.5 seconds. Position and orientation estimated using GNSS/IMU measurements are then used to provide intermediate updates of the display for the teleoperator. An experimental study involving 5 human subjects is then undertaken to compare steering control performance with and without the intermediate estimation-based display updates on curved roads. Subsequent to the submission of this preliminary conference paper, an extended version of the paper involving teleoperation with both steering control and throttle/brake control in the presence of

R. Rajamani and Gaurav Sharma are with the Department of Mechanical Engineering, University of Minnesota, Twin Cities, Minneapolis, MN 55455 USA (Email: rajamani@umn.edu; TEL:612-626-7961; sharm936@umn.edu)

other vehicles was completed, and the results are available in a journal paper that has been accepted for publication [12].

The primary contributions of this conference paper are as follows:

- The paper presents a teleoperation platform using MATLAB's Automated Driving Toolbox that provides a co-simulation environment for experimental human-inthe-loop teleoperation studies.
- 2) This paper presents an estimation-based predictive display system which uses ego state estimation to provide intermediate updates of the vehicle position with respect to its environment for improvement of teleoperator steering performance.
- 3) This paper presents an experimental human subjects study to evaluate the effectiveness of using the estimation-based display system to compensate for the degradation caused by delay. The benefits of the ego state estimation system for enhancing *steering control* are studied.

The outline of the rest of the paper is as follows. In section II, the MATLAB based teleoperation simulator is described. Section III describes the estimation-based predictive display system where state estimation of the ego vehicle is described. Section IV describes the results from a human subjects study and proves the efficacy of using estimated ego position updates to improve steering control. Section V contains the conclusions.

## II. TELEOPERATION SIMULATOR DESIGN

This section describes the teleoperator station and its components, which include a control input device that provides throttle, brakes, and steering wheel inputs from a human teleoperator, a virtual driving environment, delay control units, accurate vehicle dynamics, and realistic visual feedback of the remote vehicle environment to the human user. The MATLAB Automated Driving Toolbox has been used for developing the testing environment for human-in-the-loop teleoperation simulations and the driving scenario for the simulations has been implemented using MATLAB's



Fig. 1. Teleoperation Station

Driving Scenario Designer. Fig. 1 shows the teleoperation station used in the current work along with the computer and monitor. The monitor is a Samsung 49" Odyssey G29. The computer has 24 cores with 64 GB RAM, an Intel i9 processor, and a NVIDIA RTX 4090 24 GB graphics card.

# A. Control Input Device and Vehicle Dynamics

The Logitech G29 racing wheel along with external brake

and throttle is used to provide the control inputs which are steering angle, brake, and throttle commands. The racing wheel has 900-degree lock-to-lock rotation like a real racing wheel and provides dual-motor force feedback for accurately simulating force effects. The nonlinear brake pedal mimics the characteristics of a pressure sensitive brake system. The Joystick Input block is used as a software interface between the Simulink environment and the control commands provided by the user.

A based 34-DOF vehicle dynamic simulator based on Simulink/MATLAB which includes nonlinear tire force models has been used to simulate the actual vehicle dynamics for the ego vehicle. Using such an accurate vehicle dynamics algorithm allows simulating real-world driving while utilizing the experimental control inputs provided by the user.

## B. Delay Control Unit

The delay in the transmission of the remote vehicle environment over a wireless communication network results in latency which affects teleoperation. In particular, large size data streams which include camera images and Lidar data are more likely to be delayed during wireless transmission. The delay block in Simulink has been used to simulate this latency and thus delay the display to the teleoperator. This block can delay the display signal based on a set delay duration. Additionally, it can accommodate variable delay lengths determined by the characteristics of the local wireless network characteristics. A constant delay has been used in the current simulations.

# C. Simulink-Unreal Engine Co-simulation Environment

The MATLAB Automated Driving Toolbox's cosimulation environment employs Simulink to simulate the lateral and longitudinal positions and orientation of ego vehicle. The Unreal Engine, which is a 3D creation tool for photorealistic visualization has been used to visualize the scene in the 3D simulation environment thus acting as the visual display for the teleoperator. The vehicle dynamics uses the real time control commands of the teleoperator as inputs to provide the trajectory of the ego vehicle. This trajectory is subsequently utilized by the Scenario Reader to obtain real-time lane boundary information. The trajectory of the ego vehicle is then fed to a Simulation 3D Vehicle with Ground Following block. This block provides the position and yaw

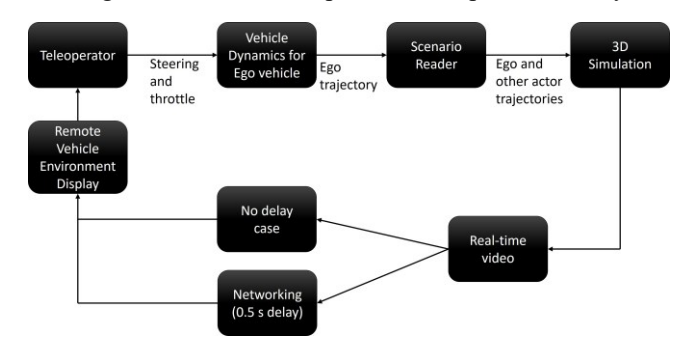


Fig. 2. Block diagram of visual display for without delay and delayed cases

angle data in the inertial frame to the Simulation 3D Scene Configuration block. In turn, the Simulation 3D Scene Configuration block renders the 3D simulation environment within Unreal Engine, providing the teleoperator with photorealistic visual feedback.

The latency in teleoperation is simulated by delaying the display of the trajectory using a delay block. The delayed trajectory is then fed to the Unreal Engine. Fig. 2 shows the block diagram of the teleoperation simulator platform for both without delay and with delay cases.

## III. STATE ESTIMATION OF EGO VEHICLE

The performance of the teleoperator is drastically affected by latency in the display of the remote vehicle environment and even a 0.17 s delay degrades control performance significantly. Hence there is a need to develop a solution to this problem. The estimation-based predictive display system developed in this paper modifies the visual feedback to the teleoperator based on intermediate updates of the state estimates of the ego-vehicle. This method offers an attractive option to enhance teleoperation. This section describes the state estimation of the ego vehicle used.

Consider an inertial frame  $(O_I, x_I, y_I)$  whose x and y axis are given by  $x_I, y_I$  and origin is located at  $O_I$ . The ego frame  $(O_E, x_E, y_E)$  is located at the center of mass (CoM) of the ego vehicle  $O_E$  and  $x_E$  and  $y_E$  are chosen to be the x and y position of the CoM of ego vehicle which is expressed in the Inertial frame. Let, the state vector X be,

$$X = [x_E \quad y_E \quad \dot{x}_E \quad \dot{y}_E \quad \psi_E]^T = [x_1 \quad ... \quad x_5]^T$$
 (1) where,  $\dot{x}_E$  and  $\dot{y}_E$  are the rate of change of  $x_E$  and  $y_E$ , respectively and  $\psi_E$  is the yaw angle of the ego vehicle.

In this paper it is assumed that the ego vehicle has an IMU which is located at its CoM and provides the following measurements that can be used as inputs by the observer,

$$u = [a_x \ a_y \ \omega_E]^T = [u_1 \ u_2 \ u_3]^T$$
 (2)

where  $a_x$  and  $a_y$  are the accelerations of the ego vehicle about  $x_E$  and  $y_E$  axis respectively and  $\omega_E$  is the yaw rate of ego vehicle. The ego vehicle with respect to (w.r.t.) the Inertial frame, the states vector, and the inputs provided by IMU are shown in Fig. 3.

The state dynamics for ego motion is as follows,

$$\dot{X} = \begin{bmatrix} x_3 \\ x_4 \\ u_1 \cos(x_5) - u_2 \sin(x_5) \\ u_1 \sin(x_5) + u_2 \cos(x_5) \\ u_3 \end{bmatrix} = f(X, u)$$
(3)

The inputs from the IMU are used in Eq. (3) to compute the state derivatives which can be integrated to obtain the desired states. The IMU suffers from the problem of drift which is a result of unknown bias and the increases the error over time. Therefore, there is a need to use other position sensor measurements to compensate for the drift in IMU. Examples of position sensors include camera, Lidar and GPS. Although camera and Lidar based odometry methods can be highly accurate but their practicality in teleoperation is limited. Such

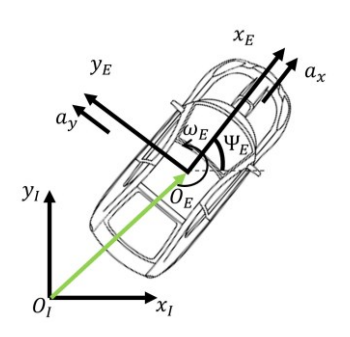


Fig. 3. Ego Vehicle w.r.t. Inertial Frame

methods consume large bandwidth due to increased data size and thus adds delay in state estimation. GPS on the other hand, has low data size and hence is a feasible option for teleoperation. However, regular GPS has low accuracy of the order of 1.5 m but when RTK corrections are used the accuracy can increase to the order of 1-10 cm. The Mn-CORS network operated by MnDOT provides RTK-corrected GPS with accuracy of 10 cm throughout the state of Minnesota. Therefore, in this work RTK corrected GPS measurements from the Mn-CORS type network has been used.

The noisy and biased measured IMU readings are related to the true signals as follows,

$$a_x = a_{x,t} + a_{x,bt} + a_{x,n} (4)$$

$$a_{v} = a_{v,t} + a_{v,bt} + a_{v,n} \tag{5}$$

$$\omega_E = \omega_{E,t} + \omega_{E,bt} + \omega_{E,n} \tag{6}$$

where,  $a_{x,t}$ ,  $a_{y,t}$  and  $\omega_{E,t}$  are the true readings,  $a_{x,bt}$ ,  $a_{y,bt}$  and  $\omega_{E,bt}$  are the constant accelerometer and gyro bias respectively and  $a_{x,n}$ ,  $a_{y,n}$  and  $\omega_{E,n}$  are zero mean white noise.

The measurement equation for the GPS is as follows,

$$y = [x_E \quad y_E]^T + v \tag{7}$$

where,  $v \sim N(0, R_{gps})$  is the measurement noise with error covariance matrix  $R_{aps}$ . Although the state is observable using the measurement in (7), but it is important to estimate yaw angle with high accuracy to improve the accuracy of the predictive display system. Hence, it is very important to use measurements of vaw angle. In literature [13], various methods have been described to compute heading which includes, using angular velocity of earth, magnetic field, vision, dual antenna GNSS, acceleration and velocity heading. Using angular velocity of earth requires costly sensors and the use of magnetic field is infeasible in AVs due to the presence of many local magnetic materials. Using vision will add latency to state estimation hence it is also not feasible. A dual antenna GPS provides accurate measurements for heading but requires a large baseline. Heading computation using velocities from GPS is a viable option as it is low cost and suitable for teleoperation. Acceleration based methods for computing heading require the differentiating velocities obtained from GPS and are thus prone to errors at low acceleration. Hence, velocities computed using GPS have been used to measure the yaw

angle.

The velocity of the ego vehicle in the inertial frame ( $\dot{x}_E^I$  and  $\dot{y}_E^I$ ) are related to those in the ego frame as follows,

$$\begin{bmatrix} \dot{x}_E \\ \dot{y}_E \end{bmatrix} = R_E \begin{bmatrix} v_x \\ v_y \end{bmatrix} = \begin{bmatrix} c_E v_x - s_E v_y \\ c_E v_y + s_E v_x \end{bmatrix}$$
(8)

where,  $v_x$  and  $v_y$  is the velocity of ego vehicle along the ego frame axis,  $c_E$  and  $s_E$  are  $\cos(\psi_E)$  and  $\sin(\psi_E)$  respectively, and  $R_E$  is the rotation matrix of ego frame w.r.t. inertial frame given by,

$$R_E = \begin{bmatrix} c_E & -s_E \\ s_E & c_E \end{bmatrix} \tag{9}$$

If  $v_r \gg v_v$ , then (8) reduces to.

$$\begin{bmatrix} \dot{x}_E \\ \dot{y}_E \end{bmatrix} = \begin{bmatrix} c_E v_X \\ s_E v_X \end{bmatrix} \tag{10}$$

Hence,

$$\psi_E = \tan^{-1} \left( \frac{\dot{y}_E}{\dot{x}_E} \right) \tag{11}$$

GPS can be used to provide  $\dot{x}_E$  and  $\dot{y}_E$  with sufficient accuracy [14] and hence this method can be used to measure the yaw angle. However, the measurements are prone to error when the lateral velocity is high (i.e., high slip angle). Hence the new measurement equation becomes,

$$y = [x_E \quad y_E \quad \psi_E]^T + v \tag{12}$$

Given these with the IMU inputs, an Extended Kalman Filter (EKF) has been used for state estimation. The prediction equations for the EKF are as follows,

$$\bar{x}_{k+1}^{-} = f(\bar{x}_k^+, u_k) \tag{13}$$

$$P_{k+1}^{-} = F_k P_k^+ F_k^T + Q_k \tag{14}$$

where,  $F_k = I_5 + \Delta t A_k$ ,  $A_k = \frac{\partial f}{\partial x}(\bar{x}_k^+, u_k)$  and  $P_k$  and  $Q_k$  are the state covariance matrix and process noise covariance matrix respectively. The correction equations for the EKF are as follows,

$$K_{k+1} = P_{k+1}^{-} H_{k+1}^{T} (H_{k+1} P_{k+1}^{-} H_{k+1}^{T} + R_{k+1})^{-1}$$
 (15)

$$\bar{x}_{k+1}^+ = \bar{x}_{k+1} + K_{k+1}(y_{k+1} - H_{k+1}x_{k+1}) \tag{16}$$

$$P_{k+1}^+ = (I - K_{k+1} H_{k+1}) P_{k+1}^- \tag{17}$$

$$P_{k+1}^{+} = (I - K_{k+1}H_{k+1})P_{k+1}^{-}$$
where,  $H_{k+1} = \begin{bmatrix} 1 & 0 & 0 & 0 & 0 \\ 0 & 1 & 0 & 0 & 0 \\ 0 & 0 & 0 & 0 & 1 \end{bmatrix}$  and  $R_{k+1}$  is the

measurement noise covariance matrix. Due to low size of GPS and IMU data, it has been assumed that the latency in the transmission of these data is negligible and the state estimation is being done on the teleoperator side.

Given the estimates of ego vehicle, the estimated vehicles were displayed to the teleoperator using the position and yaw

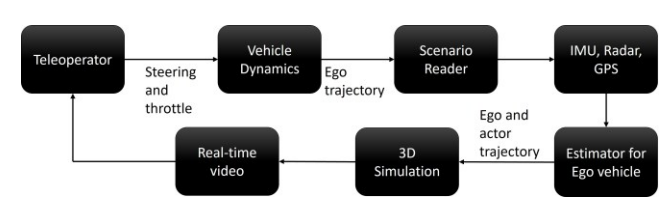


Fig. 4. Block diagram for estimation-based predictive display

angles of the vehicles. The complete flow chart of the predictive display system using state estimates is shown in

It should be noted that the vehicle dynamic model used for the ego vehicle motion is nonlinear and hence an extended Kalman filter has been utilized for state estimation in this paper. It is also possible to use nonlinear observers for such state estimation tasks [15,16], although that has not been pursued in this paper.

## IV. RESULTS AND DISCUSSION

To evaluate the performance of the estimation-based predictive display system, a human subjects study has been conducted. In this study the data of five teleoperator participants was analyzed to evaluate the degradation caused due to latency delay and the effectiveness of the predictive display system. For the human subject study, a curved road scenario was used.

The curved road extends from -200 m to 1600 m in y direction and 1400 m to 200 m in x direction as shown in Fig. 5 and has 4 lanes of width 3.85 m each. Fig. 6 shows the real-

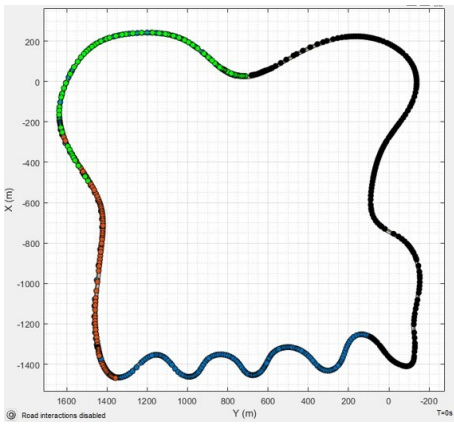


Fig. 5. Curved road scenario



Fig. 6. Real-time display to the teleoperator

time display to the teleoperator which includes the speed display (in miles per hour) along with the cockpit of the ego vehicle.

Each participant underwent three driving tests with the vehicle. In the initial test, participants operated the vehicle without any delay, while in the second test, they experienced a 0.5 second delay. The third test involved estimation-based predictive display. Each test lasted for about 6.67 mins during which the participants were instructed to maintain the ego vehicle in the same lane and drive at speeds ranging from 30 to 35 mph. Table I provides the sensor specifications of the ego vehicle which includes IMU, GPS and camera.

TABLE I. SENSOR SPECIFICATIONS OF EGO VEHICLE

Sensor Specification	Value
GPS position accuracy (m)	0.1
GPS velocity accuracy (m/s)	0.1
Accelerometer initial bias (m/s²)	0.0141
Accelerometer VRW (mg)	0.2
Gyroscope initial bias (deg/s)	0.0573
Gyroscope ARW (deg/√Hr)	0.21
GPS, IMU rate (Hz)	100
Camera field of view horizontal (deg)	56.72
Camera field of view vertical (deg)	87.66
Camera frame rate (FPS)	100

TABLE II. STATE ESTIMATION ERROR FOR EACH PARTICIPANT

Part. no.	<i>x</i> (m)		$\widetilde{y}$ (m)		$\widetilde{\psi}$ (deg)	
	RMSE	Max error	RMSE	Max error	RMSE	Max error
1	0.0114	0.0868	0.0145	0.1387	0.1169	0.6074
2	0.0116	0.0868	0.0148	0.1387	0.1227	0.5389
3	0.0114	0.0868	0.0145	0.1387	0.1088	0.4000
4	0.0115	0.0868	0.0153	0.1387	0.1867	0.8253
5	0.0113	0.0868	0.0141	0.1387	0.1025	0.4722

The state estimation results for a sample participant are shown in Fig. 7. The state estimation error is  $\tilde{e} = e - \hat{e}$ , where e is the true value and  $\hat{e}$  is the estimated value. From the plot it is clear that the error in the position and velocity is of the order of 5 cm and 5 cm/s. The error in the yaw angle is less than  $0.5^{\circ}$  indicating that the filter is able to estimate the yaw angle accurately. The state estimation error for each participant are described in Table II. The table clearly demonstrates that the estimator can achieve an accuracy of

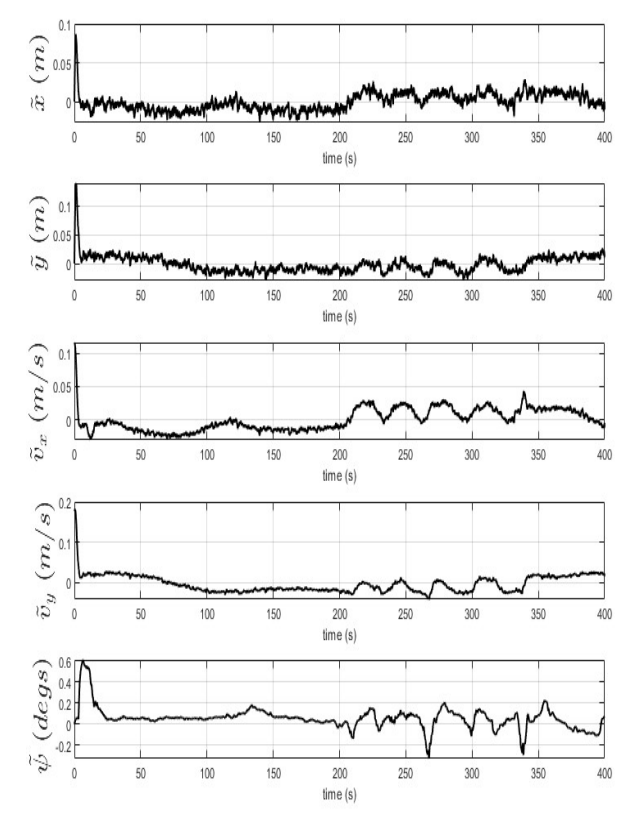
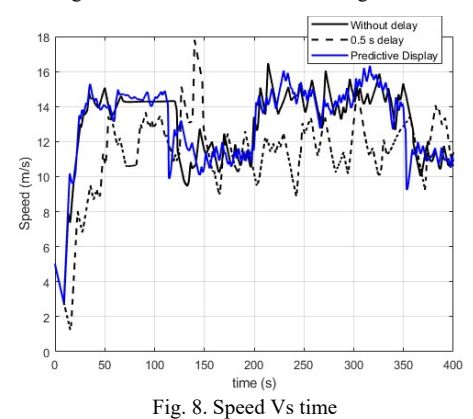


Fig. 7. Error in state estimation of ego vehicle



1.16 cm using the GPS measurements which have an accuracy of 10 cm. Additionally, utilizing the heading angle for

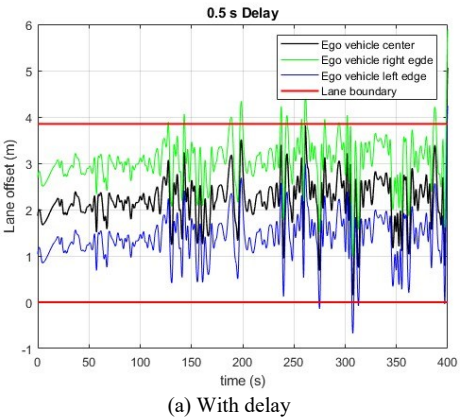
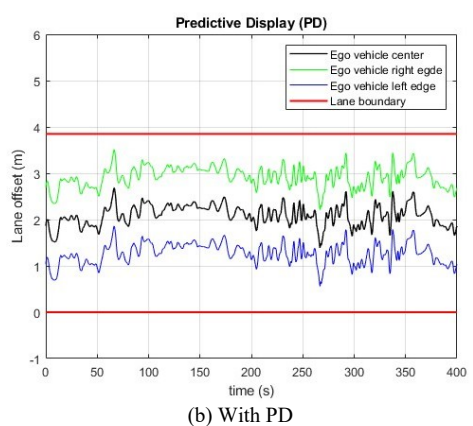


Fig. 9. Lane offset Vs Time



measuring the yaw angle results in even more precise estimation, with an accuracy of 0.1 degrees. This implies that (11) serves as a valid approximation for yaw angle measurement when the slip angle is not high.

The plot of the speed of a sample participant for all the three cases is shown in Fig. 8. From the plot it is clear that the speed of the participant for the delayed case is less than that of the without delay and predictive display cases. Moreover, the high magnitudes of variation in speeds indicates difficulty in driving the vehicle in the delayed case. The speed of the participant for the predictive display case is comparable to that of the without delay case and is higher than the delayed case indicating an improved performance in longitudinal control.

The plot for the lane offset for the ego vehicle for both delayed and predictive display case for a sample participant is shown in Fig. 9. From the plot it is clear that the ego vehicle goes outside the lane many times for the delayed case. But for the predictive display system the lane keeping performance is much better than the delayed case, thus predictive display improves the performance for lateral control.

A summary of the overall results for the human subjects study is shown in Table III. The metrics are an average over all the five participants. From the table it can be observed that both the average speed and distance covered with 0.5 s delay decreases drastically but when predictive display is used the performance is much closer to the without delay case. The table also indicates that the maximum times the vehicle goes out of lane is much less for predictive display as compared to the delayed case. The results indicate that the use of predictive display improves the longitudinal and the lateral control of the ego vehicle.

TABLE III.	RESULTS FROM TELEOPERATION STATION STUDY

Metric	Average Values			%	%
	Without delay	0.5 s delay	PD	change due to delay	change after PD
Average speed (m/s)	12.9	11.35	12.94	12	0.3
Distance (km)	5.16	4.54	5.18	12	0.39
Max distance outside lane (m)	0.064	2.39	0.084	3634	31.2
Number of times outside lane	0.4	5.2	0.4	1200	0

## V. CONCLUSION

This paper introduces an estimation-based predictive display system aimed at enhancing teleoperated steering control performance with autonomous vehicles. Teleoperation of a remote vehicle faces challenges due to latency in transmitting camera images to the teleoperation station, which can delay the visual display for the teleoperator and impact the teleoperator's performance. To assess the degradation caused in steering control by delays and the

effectiveness of the predictive display in compensating for these delays, a MATLAB-based human-in-the-loop teleoperation environment was developed. The position and yaw angle of the ego vehicle were estimated using a nonlinear dynamic motion model and an EKF based state estimation technique. The estimated states were then used in a predictive display system to synthesize images appropriately using Matlab's Unreal Engine. An experimental study involving human subjects highlighted the detrimental impact of even a 0.5 second delay in visual display on steering control. The study demonstrated that the use of an estimation-based predictive display system could effectively compensate for the delay in camera image transmissions. Steering control performance almost as good as that of the delay-free case could be obtained by using such a predictive display system.

## REFERENCES

- [1] https://news.engin.umich.edu/2020/05/delivery-robots-help-ann-arborrestaurants-weather-covid-crisis/
- [2] Gnatzig, S., Chucholowski, F., Tang, T., and Lienkamp, M. (2013). A system design for teleoperated road vehicles. ICINCO (2), 231–238.
- [3] Jessie Y. C. Chen, Ellen C. Haas, and Michael J. Barnes. Human performance issues and user interface design for teleoperated robots. IEEE Transactions on Systems, Man, and Cybernetics, Part C (Applications and Reviews), 2007.
- [4] James Davis, Christopher Smyth, and Kaleb McDowell. The effects of time lag on driving performance and possible mitigation. IEEE Transactions on Robotics, 26(3):590–593, 2010.
- [5] Frederic Chucholowski. Evaluation of display methods for teleoperation of road vehicles. Journal of Unmanned System Technology, 3:80–85, 02 2016. doi: 10.21535/just.v3i3.38.
- [6] Sato etal. Implementation and evaluation of latency visualization method for teleoperated vehicle. In 2021 IEEE Intelligent Vehicles Symposium (IV), pages 1–7, 2021.
- [7] Frederic Chucholowski. Eine vorausschauende Anzeige zur Teleoperation von Straßenfahrzeugen. PhD thesis, 03 2016.
- [8] Gaetano Graf, Hao Xu, Dmitrij Schitz, and Xiao Xu. Improving the prediction accuracy of predictive displays for teleoperated autonomous vehicles. In 2020 6th International Conference on Control, Automation and Robotics (ICCAR), pages 440–445, 2020.
- [9] Yingshi Zheng, Mark J. Brudnak, Paramsothy Jayakumar, Jeffrey L. Stein, and Tulga Ersal. Evaluation of a predictor-based framework in high-speed teleoperated military ugvs. IEEE Transactions on Human-Machine Systems, 50(6):561–572, 2020.
- [10] Henrikke Dybvik, Martin Løland, Achim Gerstenberg, Kristoffer Bjørnerud Sl'attsveen, and Martin Steinert. A low-cost predictive display for teleoperation: Investigating effects on human performance and workload. International Journal of Human-Computer Studies, 145: 102536, 2021
- [11] MD Moniruzzaman, Alexander Rassau, Douglas Chai, and Syed Mohammed Shamsul Islam. High latency unmanned ground vehicle teleoperation enhancement by presentation of estimated future through video transformation. J Intell Robot Syst, 106, 2022.
- [12] G. Sharma and R. Rajamani, "Teleoperation Enhancement for Autonomous Vehicles Using Estimation Based Predictive Display," in IEEE Transactions on Intelligent Vehicles. Accepted for publication.
- [13] Gade, K. (2016). The Seven Ways to Find Heading. The Journal of Navigation, 69(5), 955-970.
- [14] Ji, L., Sun, R., Cheng, Q. et al. Evaluation of the performance of GNSS-based velocity estimation algorithms. Satell Navig 3, 18 (2022).
- [15] Rajesh Rajamani, Woongsun Jeon, Hamidreza Movahedi, Ali Zemouche, On the need for switched-gain observers for non-monotonic nonlinear systems, Automatica, Volume 114, 2020.
- [16] A. Zemouche, F. Zhang, F. Mazenc and R. Rajamani, "High-Gain Nonlinear Observer With Lower Tuning Parameter," in IEEE Transactions on Automatic Control, vol. 64, no. 8, pp. 3194-3209, Aug. 2019.